





Effect of graphite filler on the physicochemical properties of graphite reinforced thermoset rooflite – unsaturated polyester resin composites

M. Karunakaran ^{ab} , Ravi Subban ^{b*} , A. Thangamani ^b ,
Chinnaswamy Thangavel Vijayakumar ^c 

a: Department of Chemistry, Government Arts College, Udumalpet 642 126, Tamilnadu, India

b: Department of Chemistry, Karpagam Academy of Higher Education, Coimbatore 641021, Tamilnadu, India

c: Department of Polymer Technology, Kamaraj College of Engineering and Technology (Autonomous), S.P.G.C. Nagar, K.Vellakulam 625701, Tamilnadu, India

* Corresponding author: subbanravi31@gmail.com



This paper belongs to a Regular Issue.

Abstract

It is well known that many polymers are insulators with poor mechanical properties, which limit their use in fuel cell applications. Physicochemical properties of the polymers can be improved by adding conductive fillers. Carbon-based materials like graphite, which provides excellent mechanical strength and thermal conductivity to the polymer matrices, is of special interest because of its abundance, low cost and light weight when compared to other carbon allotropes. In the present work we describe the physicochemical properties of rooflite unsaturated polyester resin/graphite composites. Rooflite resin and three of its composites containing 1%, 3% and 5% of graphite by weight (C-2, C-3, and C-4, respectively) were synthesized and characterized by FTIR spectral data. XRD showed two peaks at $2\theta = 27.37^\circ$ and 55.40° with d spacing value of 3.2559 nm and 1.6571 nm, respectively, indicating the change in degree of crystallinity of the composite. The calculated crystallinity for the resin is 7.3%, and for C-2, C-3 and C-4 its values are 12.1%, 14.3%, 17.1%, respectively, evidencing the interactions between the graphite and polymer matrix. The composites showed fractured surfaces and porous rough structure with randomly distributed vascularized cavities. Agglomeration occurs, when the concentration of graphite increases. The glass transition temperature for the pure resin is 65.9°C and increases when the resin is filled with graphite. Thermogravimetric analysis (TGA) of the composites showed no marked difference between T_{max} and T_{final} , and LOI values of C-3 and C-4 are above 21%, making them self-extinguishable materials that could be used for making bipolar plates. The chemical resistance investigation against water, NaCl, NaOH, acetic acid, and toluene showed more resistance to acid than alkali solutions. These rooflite resin/graphite composites could be further studied to explore the possibility of making bipolar plates, which are an essential component of fuel cells.

Keywords

rooflite
unsaturated polyester resin
graphite
composites
morphology
thermal properties
chemical resistance study

Received: 24.01.24

Revised: 09.02.24

Accepted: 09.02.24

Available online: 29.02.24

Key findings

- The crystallinity index of the studied composite materials increased due to the enhanced interaction between the resin matrix and graphite filler.
- Agglomeration due to higher concentration of graphite filler lowers the interfacial contact and affects the mechanical characteristics of the composites.
- The glass transition temperature increases with the addition of graphite.
- When the percentage of graphite in composites is raised, the limiting oxygen index revealed that the composites are self-extinguishing.
- The synthetic composites exhibit a consistent swelling behavior in response to different chemical environments.

© 2024, the Authors. This article is published in open access under the terms and conditions of the Creative Commons Attribution (CC BY) license (<http://creativecommons.org/licenses/by/4.0/>).

1. Introduction

Unsaturated polyesters containing olefinic unsaturation are produced by a condensation reaction between polyols and polycarboxylic acids with an acid reactant. The polyesterification reaction between bifunctional acids like phthalic acid, maleic acid, etc., with bifunctional alcohols like glycols results in a highly viscous unsaturated polyester along with water as a by-product, which is directly removed from the reaction mass [1]. To reduce the viscosity of the unsaturated polyester, it is dissolved in a monomeric solvent of low viscosity comprising styrene with carbon-carbon double bonds, and methyl methacrylate. The resultant product is called unsaturated polyester resin. Such unsaturated polyester resins are macromolecules with a polyester backbone and belong to a category of thermoset resins. During the formation of an unsaturated polyester resin, the reaction between the carbon-carbon double bonds of the unsaturated polyester and the monomer is facilitated by a radical-initiated polymerization reaction, which is called curing or cross-linking. Organic peroxides like methyl ethyl ketone peroxide (MEKP) are widely used as catalysts or initiators for the curing process at room temperature. The accelerator employed for this curing process is cobalt salts [2].

Composite materials are synthesized by mixing or reinforcing a core material, referred to as the base material, in a certain proportion with one or more filler materials, referred to as matrix materials. Innumerable composites are produced using various thermosetting matrix resins. Unsaturated polyester resin is one among them [3]. A variety of filler materials are used to produce unsaturated polyester composites. Some of the natural materials based on carbon are also used as fillers. Carbon-based conductive fillers like Carbon black [4], graphite powder, and expanded graphite (EG) [5] are used to generate polymer composites for several applications. Since graphite is the cheapest material, it has a typical layered structure, possesses good electrical and thermal conductivity, has good chemical stability, and is widely used in polymer/graphite composites.

The dynamic mechanical and thermal properties of unsaturated polyester resin composites synthesized using unsaturated polyester resins and modified or unmodified graphite were studied and reported [6]. The synthesized unsaturated polyester resin with graphene nanosheet composites possesses enriched electrical, mechanical, and thermal properties [7]. When the unsaturated polyester resin matrix is composited with graphite nanosheets as filler material, the resultant composite has decreased polymerization shrinkage. However, the electrical and thermal conductivity and glass transition temperature of unsaturated polyester resin composites are increased [8]. The improved mechanical properties such as tensile strength, elongation at break, and hardness were reported for unsaturated polyester resin with nanocarbon composites [1]. An increase in the percentage weight of aluminum and graphite as rein-

forcing materials improves the hardness, impact, and tensile strength of unsaturated polyester resin composites. Various graphene-filled unsaturated polyester resin composite and graphite-filled unsaturated composites were synthesized, and the thermal properties of those composites were evaluated using differential scanning calorimetry (DSC). The results show that the specific heat value of polyester composites with graphene is 10% higher than that of polyester composites with graphite [9]. The mechanical and thermal properties of composites synthesized by using either graphene oxide or graphite as a filler material with an unsaturated polyester matrix were reported. The increase in the glass transition temperature, determined with the help of dynamic mechanical analysis for both composites, was observed when compared with pure resin.

The brief literature review can be summarized as follows: only a few notable works on unsaturated polyester resins and graphite composites have been reported to date. The synthesis of rooflite-unsaturated polyester resin/graphite composites is explained in detail in this work. The explanation is based on the dispersion of various concentrations of graphite in rooflite resin. The criteria that are studied in detail and reported include the chemical structure, crystallinity, morphology, and thermal stability. The abovementioned properties of the synthesized composites were reported.

2. Materials and Methods

2.1. Materials

The materials—rooflite polyester resin, accelerator, and catalyst—were purchased from S.R. Resins, Coimbatore, Tamil Nadu, India. The resin was synthesized through a process called condensation. The procedure is done using propylene glycol, monoethylene glycol, phthalic anhydride, and maleic anhydride at a temperature of 230 °C. The above-mentioned procedure is depicted in the figure below. The result obtained from the previously quoted synthesis is 60% solid, which is to be dissolved in 10% methyl methacrylate and 30% styrene. Hence, the results of the analysis can be put forward as rooflite resin has a viscosity of 550±100 CPS, acid number mg KOH/gm of 24.0±4.0, and gel time of 16–24 min. The products used to carry out this mentioned analysis are 0.2% cobalt naphthanate (6% Co content) as an accelerator and 50% methyl ethyl ketone peroxide (MEKP) diluted with hydrogen peroxide as a catalyst. Graphite Fine Powder (98%) Extra pure was provided by Loba Chemicals Private Limited, India.

2.2. Preparation of rooflite resin / graphite composites

The preparation of the composite can be described clearly in this procedure. The composite incorporated can be made by combining the required amount of rooflite resin with cobalt naphthenate (1 ml per 100 g of resin) and graphite

powder under mechanical agitation. The dispersion obtained from the previously described process was subjected to ultrasonication at room temperature for about 1 hour. After that, the same was degassed. Next, the addition of a desirable quantity of methyl ethyl ketone peroxide (MEKP) (1 ml per 100 g of resin), which acts as an initiator, was carried out. This sample was subjected to rapid stirring and transferred to a glass mold. The procedure of stirring was performed to avoid the formation of air bubbles. The pouring of the sample into the glass mold was preceded by yet another step. Mansion wax polish was used to coat the inner surfaces of the glass mold before pouring the sample. After this, the composite sample within the glass mold was cured at room temperature for about 24 h. Following the process of curing, yet another process of post-curing was carried out in a hot air oven at about 80–90 °C for approximately 2 h. After completion of the entire procedure, the hot glass mold with the composite was allowed to cool to room temperature. The removal of the composite from the glass mold was done after desiccation. The synthesis procedure is shown in Figure 1. The percentage of graphite added to rooflite resin is shown in Table 1.

2.3. Characterization

The major method used for analysis is the IR-spectroscopic technique. The findings obtained using the abovementioned technique are the chemical nature and functional group investigation results for the graphite powder, pure rooflite resin, and composites. The IR spectra of all the samples were recorded in ATR mode, from 4000 cm^{-1} to 400 cm^{-1} . A Bruker alpha II-FTIR spectrometer was utilized for this analysis. XRD analysis was also performed to assess the crystallinity of graphite and composites. An advanced Bruker D8 diffractometer was employed to collect X-ray diffraction patterns in copper radiation with the wavelength of 1.54 Å. The patterns were obtained at 40 kV and 40 mA, with a scan rate of 0.02° s^{-1} , and at $2\theta = 10\text{--}70^\circ$. The crystallinity index (Cr.I.) was calculated using the peak height method from reflected intensity data [10], and [11] according to Equation (1):

$$\text{Cr.I.} = (I_{020} - I_{\text{am}}) / I_{020}, \quad (1)$$

where I_{020} is the maximum intensity of the lattice diffraction and I_{am} is the intensity at $2\theta = 18^\circ$ for the amorphous region.

The TESCAN VEGA3 SBH tungsten thermionic emission SEM system of resolution 2 nm was used to obtain better knowledge of the morphology of the synthesized composites. A NETZSCH DSC 350 SIRIUS system with Proteus software was used for the study of the glass transition temperature (T_g). Differential scanning calorimetry (DSC) method was employed in a nitrogen atmosphere at a scan rate of 10 °C min^{-1} . NETZSCH, model NJA-STA 2500 Regulus is an instrument used for thermogravimetric analysis of the thermal degradation of graphite, rooflite resin, and their composites. In highly pure nitrogen atmosphere, thermograms were recorded for approximately 1 to 2 mg of all

samples. The gas flows were as follows: purge gas, 40 ml/min, and working gas, 60 ml/min (a total of 100 ml/min). The measurements were performed in an Al_2O_3 crucible.

2.4. Chemical resistance study

The testing ensures whether the unsaturated polyester resin and three of its composites, C-2, C-3 and C-4, in bulk or on the surface are "resistant", "partially resistant", or "not resistant" to a certain chemical over a predetermined length of time. In this study, the change in weight of the pure rooflite resin and its graphite composites were determined before and after immersion in respective solvents or solutions. The chemical resistance of the pure resin plates and composite resin plates was measured three times. This method used 5 solvents: water, 10% sodium chloride solution, 10% sodium hydroxide solution, acetic acid solution (5%), and toluene solution. Before the plates were submerged in the solvent/solvent, they had been carefully cleaned with filter paper and weighed. After that, the plates were submerged in the respective solution/solvent for approximately 168 h (1 week). After one week the immersed plates were removed from the solution/solvent, carefully cleaned with filter paper, air dried and then weighed. The arithmetic mean of the three weight values acquired for the three samples, following the same amount of immersion time, were used to get the end result. The test plate dimensions are 2x2x3 cm according to ASTM Standard D543.

3. Results and Discussion

3.1. Fourier transform infrared (FTIR) studies

Based on the scale for the given segment, between 4000 cm^{-1} to 650 cm^{-1} , Fourier transform infrared (FTIR) spectrum of pure rooflite resin denoted as C-1 is shown in Figure 2. The peaks in the IR spectrum include those at 3027 cm^{-1} , 1597 cm^{-1} and 1488 cm^{-1} . The cause of formation of these peaks is the C–H stretching of an aromatic ring [12]. The peaks at 2924 cm^{-1} and 1448 cm^{-1} correspond to the stretching vibration of the methyl group [13]. An essential and unique band at 1726 cm^{-1} is noticed, which is contributed by an unsaturated polyester resin.

The IR spectrum of rooflite resin is in agreement with the results of the previous work [14]. An absorption peak is estimated at 1394 cm^{-1} , which is indicative of the methyl group's asymmetric bending vibrations of C–H bonds. The abovementioned phenomenon can also be manifested at 1373 cm^{-1} [15]. A noticeable peak is labeled at 1262 cm^{-1} , which is a result of the C–O stretching vibration of an ester group [16].

Table 1 Graphite (%) present in various samples studied.

Sample code	wt.% of graphite added
C-1	0
C-2	1
C-3	3
C-4	5

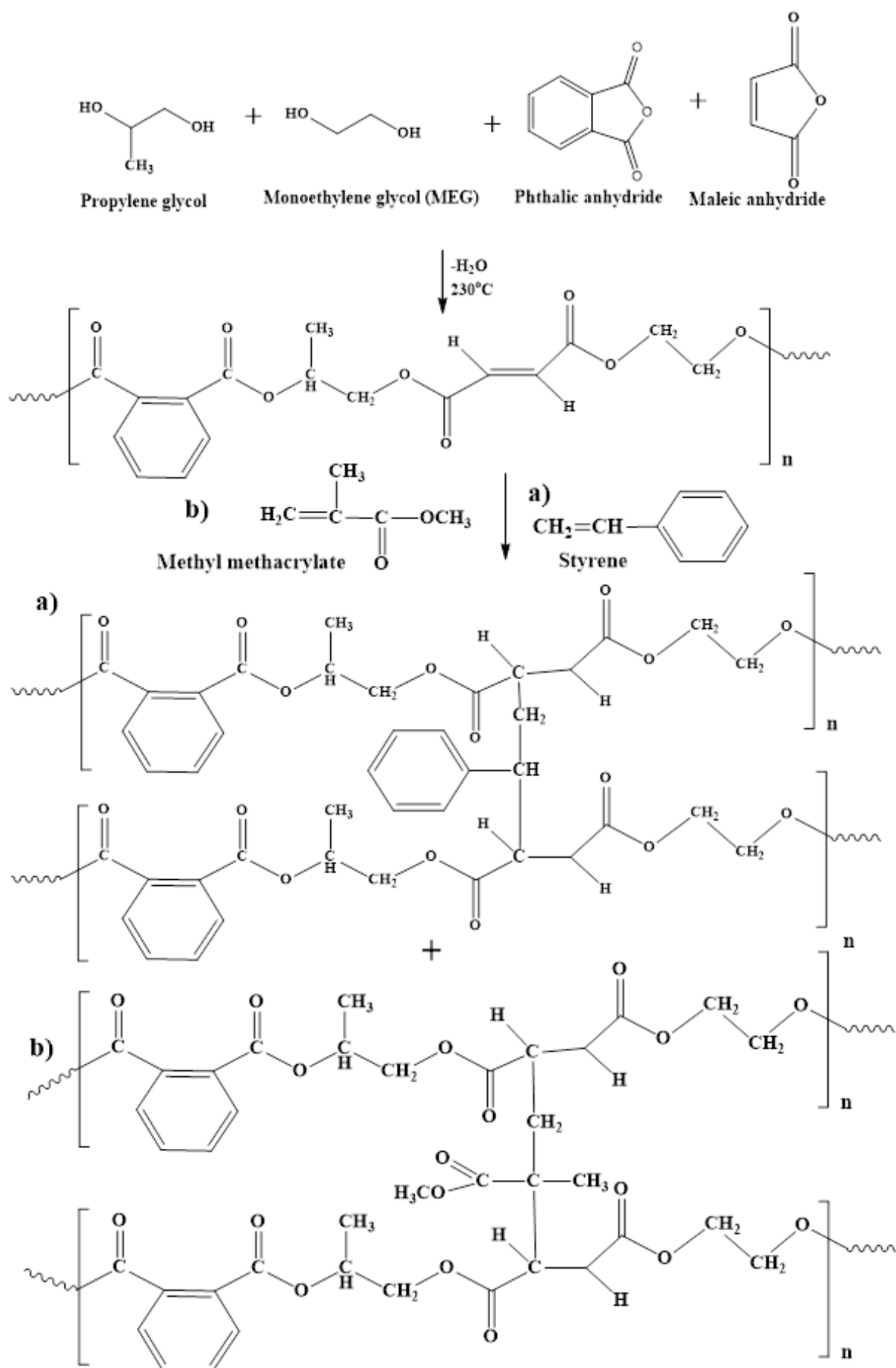


Figure 1 Synthetic process of rooflite unsaturated polyester resin.

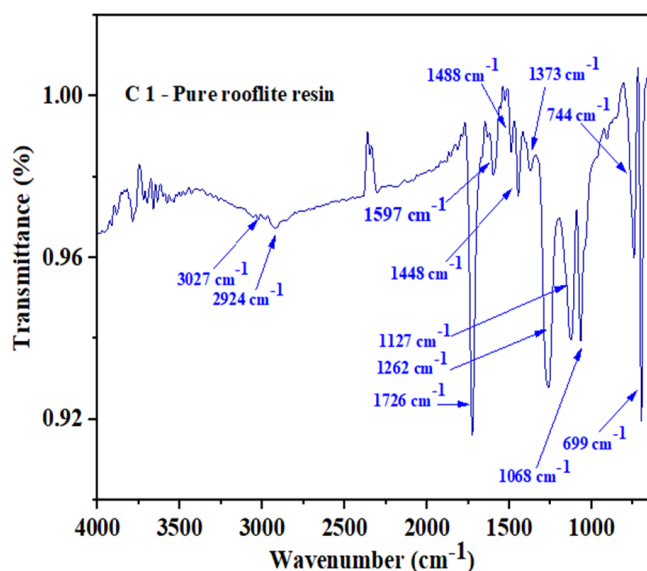


Figure 2 Fourier-transform infrared (FTIR) spectrum of pure rooflite resin.

At 1068 cm^{-1} , the asymmetric stretching vibration of C–O–C groups of the polyester segment is marked. The above-mentioned analysis is also confirmed elsewhere [17]. Distinctive, intense peaks are located at 744 cm^{-1} and 699 cm^{-1} . The prime cause for this peak formation is the out-of-plane bending of trans $-\text{CH}=\text{CH}-$ fraction. Similar peaks were also identified in the literature in the rooflite resin IR spectrum [18].

Fourier transform infrared (FTIR) spectra of graphite, pure rooflite resin tagged as C-1, and its composites with graphite containing 1%, 3%, and 5% by weight are denoted as C-2, C-3, and C-4 respectively, as shown in Figure 3. A few of the markedly weak peaks are not seen in Figure 3 due to the scale of the figure. Considering the IR spectrum of graphite, the purity of the sample is confirmed by the absence of any noteworthy peaks [18, 19].

In consideration of the FTIR spectrum of rooflite-graphite composites, the resins termed C-2, C-3, and C-4 are found to be almost identical. Peaks at 3027 cm^{-1} , 1597 cm^{-1} , and 1488 cm^{-1} are due to C–H stretching vibration. The FTIR spectrum of all of the composites illustrates the previously mentioned statement. Two peaks at 2924 cm^{-1} and 1448 cm^{-1} result from the stretching vibration of the C–H moiety present in the methyl group.

An absorption band at 1726 cm^{-1} is identified, which corresponds to the carbonyl stretching of an ester moiety. The same is true for every single rooflite resin–graphite composite. The peak at 1373 cm^{-1} is due to the asymmetric bending vibrations of the C–H bonds of the methyl group. The peak at 1394 cm^{-1} represents the asymmetric bending vibrations of C–H bonds of the methyl group. The peak at 1262 cm^{-1} corresponds to the C–O stretching vibration of an ester group. The peak at 1068 cm^{-1} indicates the asymmetric stretching vibration of C–O–C groups of the polyester segment. The peaks at 744 cm^{-1} and 699 cm^{-1} result from the out-of-plane

bending of the trans-CH segment of the resin. These peaks further indicate the presence of unsaturation in the polymer composites. Regarding the pure resins, C-1, factors such as carbonyl stretching vibration, aromatic skeleton vibration, stretching, bending vibration of a methyl group, and the presence of unsaturation are found analogous.

3.2. X-ray diffraction studies

Figure 4a represents the X-ray diffraction pattern of graphite recorded at 2θ between 0° and 70° . A peak at $2\theta = 26.46^\circ$ is exhibited by the XRD pattern, which is utilized in this analysis. The same d -spacing value of 3.3658 nm contributes to the reflection of the plane (002) [20]. Similarly, a peak at $2\theta = 54.62^\circ$ is exhibited by the crystalline nature of the graphite powder. In addition to the above, the reflection of the plane (004) is highlighted by the same d -spacing value of 16.789 nm [21].

Figure 4b shows the X-ray diffraction spectrum of pure rooflite resin and its graphite composites. The diffractogram of pure rooflite resin designated as C-1 shows one broad peak around $2\theta = 22.14^\circ$ with a d -spacing of 4.0118 nm and another broad peak around $2\theta = 43.23^\circ$ with a d -spacing of 2.0911 .

These broad peaks reveal that there is an intermolecular interaction between the long polymeric chains present in the rooflite resin. One specific detail was observed in this study. Due to such interaction, this resin structure may have several crystal defects [22]. The diffused scattering pattern and the broad peak in the diffractogram conform to the amorphous nature of the rooflite resin [23]. While the diffractogram of composite C-2 which is rooflite resin containing 1% graphite is similar to that of pure rooflite resin, it fails to expose any peaks. However, the diffraction pattern of C-2 seems too similar to that of C-1, albeit there is a minor change in peak position and increases in the d spacing values of the composites. Concerning the earlier reports, the d spacing value for pure rooflite resin is 4.0 nm [24].

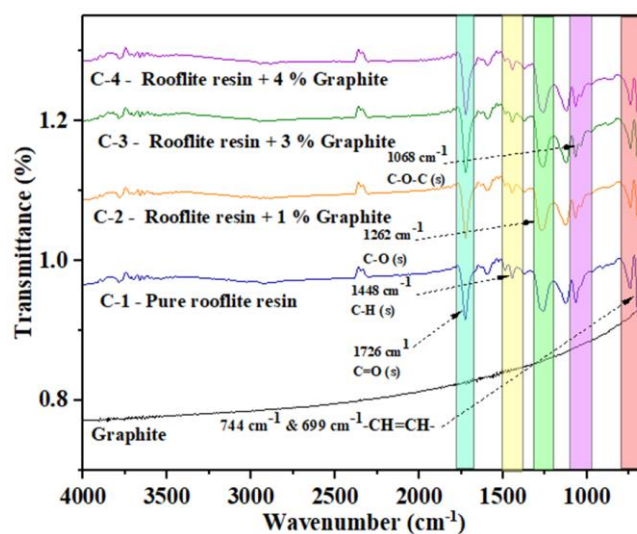


Figure 3 Fourier-transform infrared (FTIR) spectra of graphite, pure rooflite resin and its graphite composites.

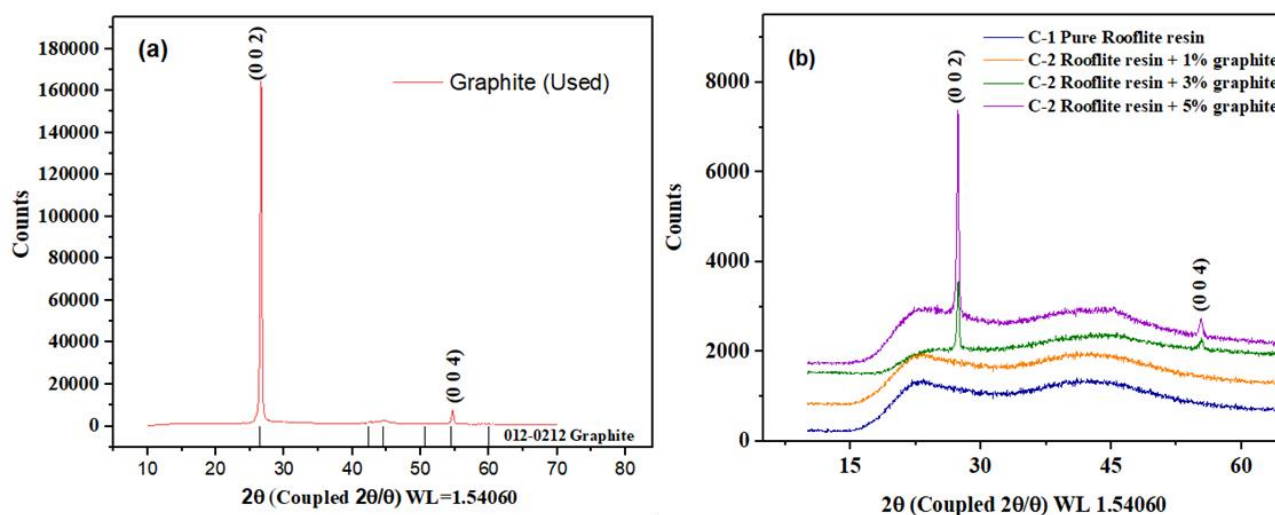


Figure 4 XRD spectrum of graphite (a), rooflite resin and its graphite composites (b).

The calculated d spacing value for C-2 is 4.1052 nm with 2θ values of 21.63. Hence, the addition of graphite in the pure rooflite resin changes the amorphous nature to semi-crystalline due to the formation of molecular symmetry after polymerization [24]. The diffraction pattern of the other two composites, designated as C-3 and C-4 and containing 3% and 5% graphite, respectively, appears to be a combined pattern of both graphite and pure rooflite resin. The diffractograms of C-3 and C-4 composites also show two distinct peaks. The addition of graphite in the polymer matrix is accountable for these two peaks. The two peaks at $2\theta = 26.46^\circ$, and $2\theta = 54.62^\circ$ are expected. Both C-3 and C-4 show first peaks at $2\theta = 27.37$ with a d -spacing value of 3.2559 nm and the second peak at $2\theta = 55.40$ with a d -spacing value of 1.6571 nm, which indicates the change in the degree of crystallinity of the composite. The small changes in the peak positions is ascribed to either expansion or contraction of the polymer lattice due to the modification of filler graphite content in the composites, which leads to stress against the filler added in the composites [25]. From the height ratio between the intensity of the crystalline peak (I_{002}) and the amorphous height (I_{am}), the crystallinity index was calculated. The graphite used in this study has a 69.8% crystalline nature. The calculated crystallinity for pure rooflite resin designated as C-1 is 7.3%. The calculated composite crystallinity for C-2, C-3, and C-4 are 12.1%, 14.3%, and 17.1%, respectively. Examining the crystallinity index values of these composites shows that there is an evident interactions between the graphite crystals and the polymer matrix. From the above results, it is observed that the crystallinity index for graphite is very high when compared with that of pure rooflite resin. When composites are synthesized using graphite and rooflite resin, the interaction between the resin matrix and filler increases. It is supposed that in composites with 1, 3 and 5 wt.% of graphite, the reinforcement encouraged nucleation sites of atomically ordered regions, which increased the crystallinity index of these composite materials [26].

3.3. Morphology

The pure graphite was used as a filler material in this study. The morphology of graphite was established with the aid of SEM images, which are shown in Figure 5. From these images, it is clear that graphite possesses a layered planar structure [27]. Every layer is made up of carbon atoms which are organized in a honeycomb lattice. Both lattices are separated by 0.142 nm, and the interplane distance is 0.335 nm. Furthermore, the graphite layers appear to be dense, which suggests that the filler is not a single-layered structure but is in the cluster. Additionally, the individual particles of graphite is visualized as having an irregular, flaky appearance [28]. The size of the graphite used in this work is approximately 5 μm . Irregularities, in association with the shapes of the particles, are identified with the number of edges, which was revealed by the two different zoomed-in images of graphite particles [29]. The SEM images for pure rooflite resin designated as C-1 are depicted in Figure 6 (C-1 a, C-1 b and C-1 c at low, medium and high magnification, respectively). In Figure 6, C-1 a, the slim streaks are seen. The surface morphology of the pure rooflite resin is smooth and flat [26]. The fractured surface of unsaturated polyester resin possesses a large number of linear gullies and warped edges, which explains the low crosslinking density of the resin when the resin is cured. The lower cross-linkage between one layer of rooflite polymer chains with another layer of the same or other atoms or molecules, it affects mechanical properties like brittleness [30]. The brittleness of the rooflite resin is also due to the cracks noticed in these pictures, which are unidirectional [31].

The mechanical properties of composites depend on the nature, shape, and properties of filler materials that are added to them. Since the filler material graphite has a huge specific area and is highly irregular in shape with the number of edges, graphite has a high interaction with the polymer matrix. Therefore, the interfacial adhesion of graphite to the resin matrix is also very high, thereby affecting the mechanical properties [32].

Synthesizing the composite plates by dispersing graphite as filler in the rooflite resin matrix presents some challenges. Figure 7 reveals that the addition of filler graphite will affect the surface morphology, making the surface less smooth. Due to Van der Waal's interaction between filler particles and the high surface energy, achieving the uniform distribution of graphite in the resin matrix is very difficult. When the concentration of filler graphite is increased, agglomeration results instead of uniform distribution of the filler [33]. The fractured surface images of composite designated as C-2 (a, b and c) containing 1% weight of graphite reveal that the smoothness of the pure resin surface is lost, being replaced by ripple texture and asymmetry. However, it is clear that the graphite filler is completely penetrated at the hetero junctions when the filler concentration is comparatively low [34]. The SEM images of composites C-3 and C-4 containing 3 and 5 wt.% of graphite displayed a rough surface structure, which is due to the modification in the microcracks with almost randomly distributed vascularized cavities. Over the surface of the composites, the filler graphite particles are visualized as clusters. When the filler concentration is increased, the surfaces of the fractured structure of the composites have a porous, rough structure with randomly distributed vascularized cavities.

If the number of sinters increases, it may lead to a change in the microcracks, which results in several void formations in the resin matrix, which, in turn, affects the properties of the composites. From Figure 7, C-4 (b), a cleavage type of surface is seen when the composite contains a graphite filler concentration of 5%, which indicates

the insignificant plastic nature of the composite [35]. The shear cups are visualized by shearing the resin matrix when graphite concentration is increased [36]. Agglomeration results when the concentration of microfiller graphite increases. Such a result was reported by Sanchez-Garcia et al., in 2010 [37]. The previously explained agglomeration can also be acknowledged in the reduction of interfacial contact between the fillers and the matrix. Thus, this results in poor interfacial stress transfer. Eventually, it affects the mechanical properties of the composites.

3.4. Differential scanning calorimetry

Rooflite resin and its graphite composites were subjected to DSC analysis. The analysis was carried out in a nitrogen atmosphere. The results are provided in Figure 8 and Table 2. From Figure 9, it is clear that all the curves are more or less similar. Every DSC curve has one endothermic and one exothermic peak since their phase transition manner is consistent [38].

The exothermic peak is attributed to the enthalpy of the cross-linking reaction, which has occurred at low temperatures with faster curing rates and a shorter time [8].

The glass transition temperature (t_g) and specific heat capacity (ΔC_p) calculated by using the Proteus software are given in Table 2. The glass transition temperature for pure rooflite resin is 65.9 °C which is the lowest value among the materials under this study. The glass transition temperature increases with graphite concentration [39]. It is also due to the fact that when graphite content increases, the relative concentration of styrene-methyl methacrylate decreases [40].

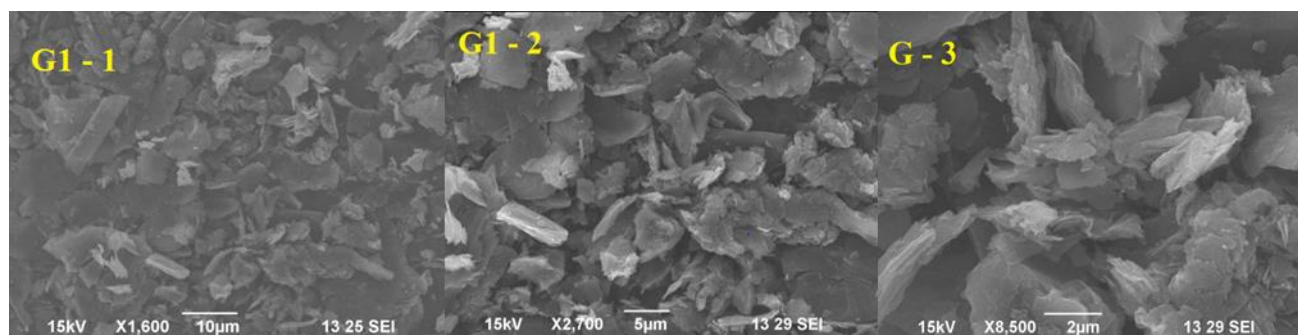


Figure 5 Low (left), medium (middle) and high (right) magnified SEM images of graphite.

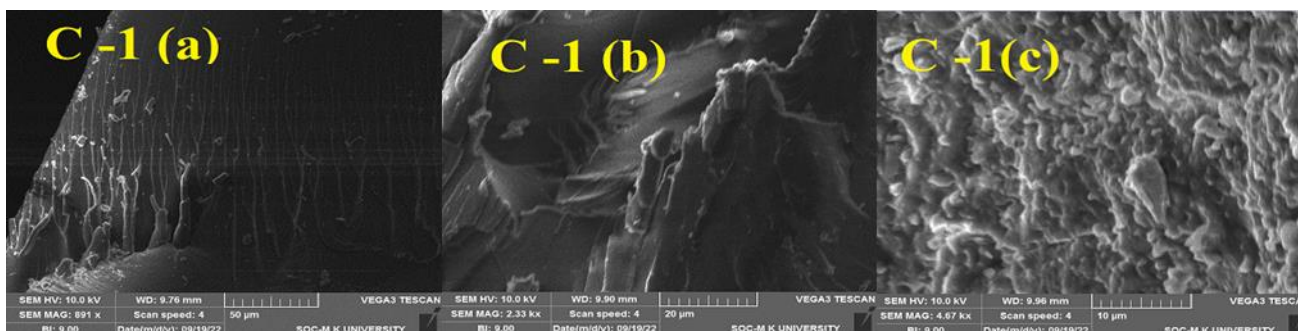


Figure 6 Low (left), medium (middle) and high (right) magnified SEM images of pure rooflite resin designated as C-1 (a), C-1 (b) and C-1 (c), respectively.

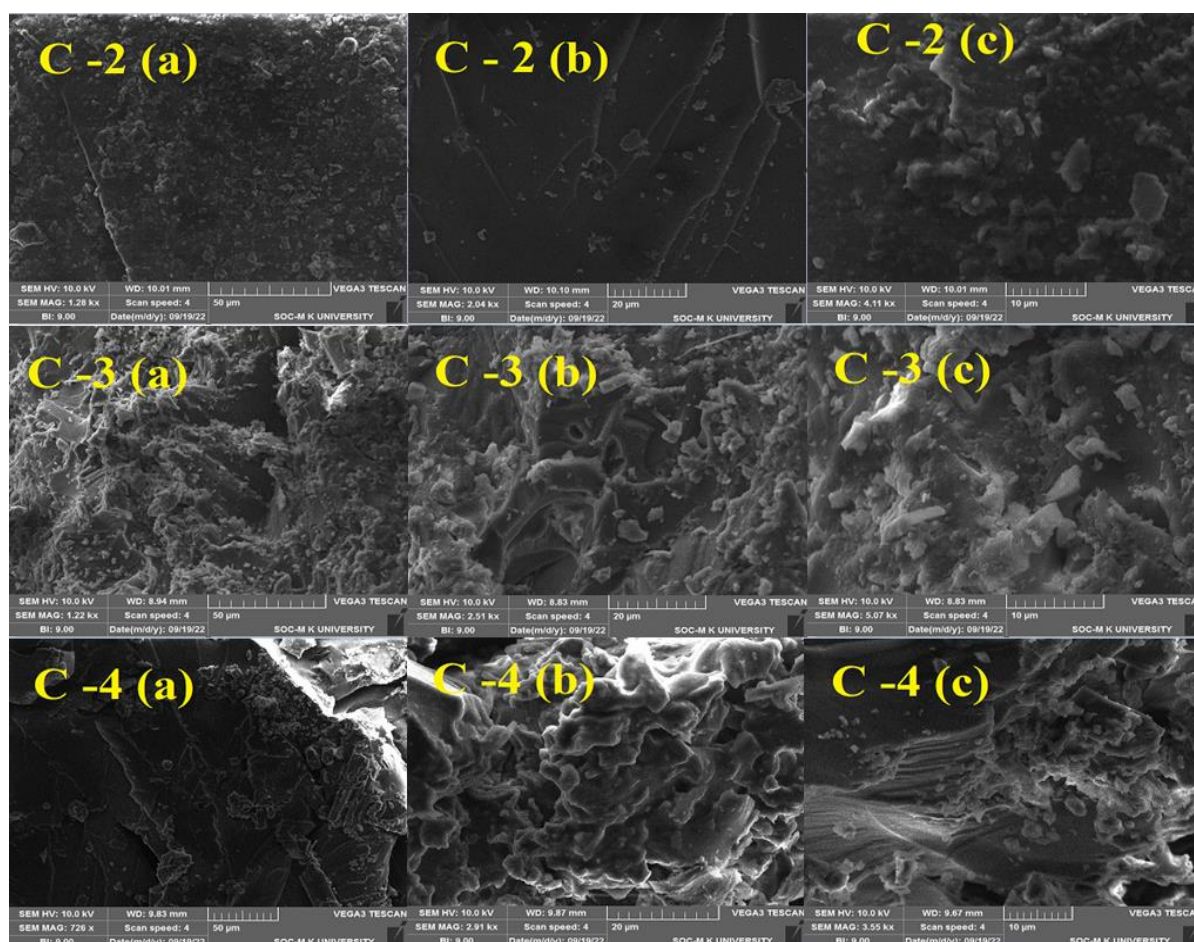


Figure 7 Low (left), medium (middle) and high (right) magnified SEM images of rooflite resin – graphite composites. C-2, C-3, and C-4 are rooflite resin composites with 1, 3, and 5 wt.% of graphite, respectively.

Identical behavior was observed for unsaturated polyester resin/expanded milled-graphite filler composites [41]. The varying degrees of interaction between the graphite filler and the unsaturated polymer resin matrices are responsible for the rise in the glass transition temperature [41]. Further Van der Waals bonds may be formed between the unsaturated polyester matrix and graphite filler [42]. Another reason for such an increase may be that graphite filler reduces segmental motion between polymer chains [9, 43]. Since the glass transition temperature acts as a threshold for the use of materials and the establishment of operational limits, its precise determination and prediction are essential.

3.5. Thermogravimetric analysis and derivative thermogram

The thermogravimetric analysis was carried out in a nitrogen atmosphere. The results for the pure resin and its graphite composites are provided in Figure 9a.

An analysis of the plot of the rate of material weight change upon heating vs temperature is called derivative thermogravimetry (DTG). It can be utilized for gaining knowledge on the thermogram peaks, which are obtained by plotting the weight versus temperature. This method simplifies the reading of the closely related thermogram peaks.

Table 2 DSC results for rooflite resin and its graphite composites.

Sample code	Graphite, wt. %	T_g (°C)	$\Delta C_p/J/(g \cdot ^\circ C)$
C-1	0	65.9	0.097
C-2	1	66.4	0.010
C-3	3	67.2	0.031
C-4	5	68.4	0.038

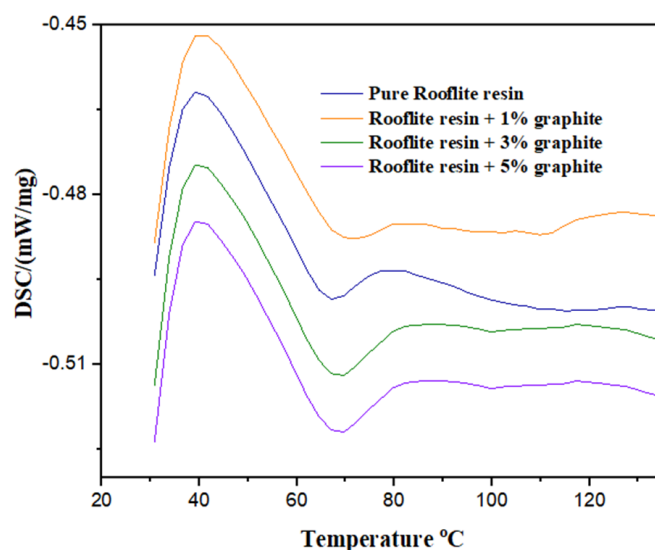


Figure 8 DSC thermogram of rooflite resin and its graphite composites.

The derivative thermogram of rooflite resin and its graphite composites is shown in Figure 9b, and the corresponding results are given in Table 3. Two values of temperature can be noted and given as T_{initial} and T_{final} . For pure rooflite resin, T_{initial} is above 300 °C whereas for the composites it is below 300 °C. Both pure resin and its composites show no marked difference between T_{max} and T_{final} . The decomposition pattern for both rooflite resin and its composites appears to be very similar. The TGA graph supports this statement, since the graphite is less reactive than the rooflite resin as it started to oxidise at higher temperatures, i.e. about 600 °C [44, 45]. The natural graphite has an endset oxidation temperature (T_e) of almost 860 °C. It is implied that the thermal breakdown process of rooflite polyester resin graphite composites is not significantly impacted by graphite at low concentrations, between 1 and 5 wt.%. Nevertheless, as Figure 9a illustrates, there is a difference in the onset temperature at which weight loss starts. It was reported that, as mass loss gets greater than 50%, graphite has an impact on how polymer composites degrade, i.e., the mass loss is decreased when the proportion of graphite in the composites increases.

DTG also provides information about single-stage thermal decomposition. The thermal degradation mechanism is not affected by the incorporation of graphite in the rooflite resin matrix. The degradation of the resin begins above 260 °C. Above 300 °, the weight loss is very high. It is attributed to the chain scissoring of unsaturated polyester resin. Fragments such as polyester and polystyrene moieties are responsible for this weight loss [46]. Moreover, the percentage increase in char yield for composites designated

as C-3 and C-4, means the residual char should be stable at this temperature at an inert atmosphere [47].

Even at 700 °C a char yield of 15.74% was observed for composites designated as C-4, which means the resultant char may serve as an effective barrier to hamper mass transfer, contain thermal conductivity, and then hinder the exothermic reaction.

Therefore, the flammability will be significantly reduced by the interference of the char [48]. The filler material expresses no catalytic activity. It is found that there is an increase in the percentage of char at 700 °C for the composites designated as C-3 and C-4 and a decrease in the same temperature for the composite designated as C-1. The % of char that measures the ignition resistance of the specimen can be assessed by calculating the Limiting Oxygen Index (LOI), which is one of the standard assessment for this purpose [49, 50].

The method to calculate LOI was proposed by Van Krevelen. This method uses the amount of char formed by the halogen-free polymers to provide desirable results. LOI is defined as the minimum concentration of oxygen in a mixture of oxygen and nitrogen that is required to maintain combustion after ignition [49]. The unit for LOI is expressed in volume percentage (vol.%). 21% of oxygen is contained in the atmosphere. The materials can be classified into two categories based on the LOI values: combustible materials and self-extinguishable materials. The former exhibits an LOI value of less than 21%, whereas the latter exhibits the same value of more than 21%. A simple equation, $\text{LOI} = 17.5 + 0.4(\text{CY})$, is implemented in the LOI technique, where CY indicates char yield.

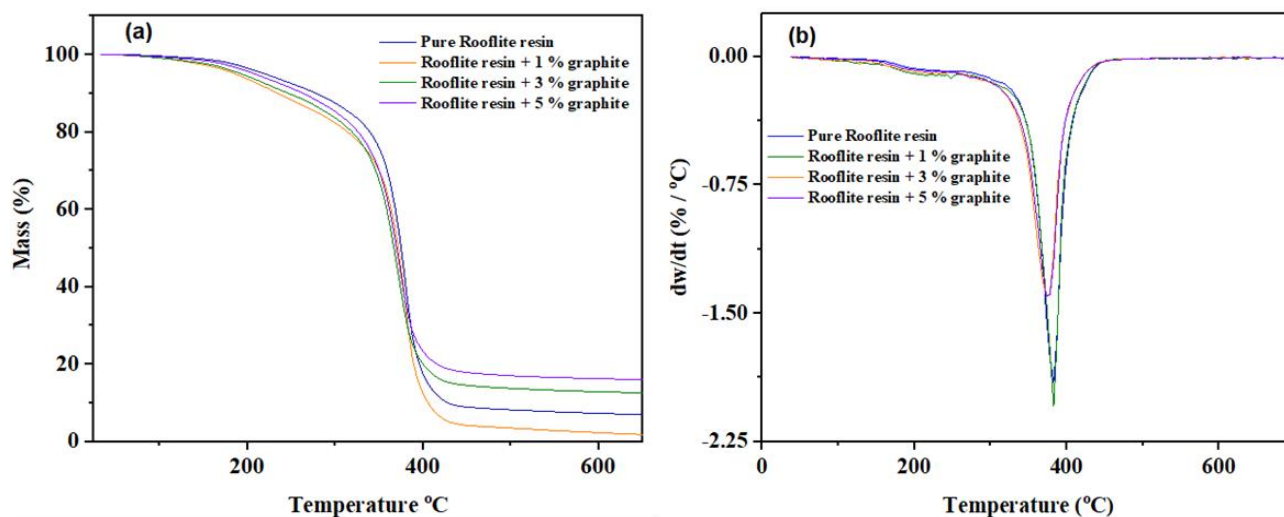


Figure 9 Thermograms of rooflite resin and its graphite composites: TGA (a) and DTG (b).

Table 3 Thermogravimetric analysis results for rooflite resin and its graphite composites.

Sample code	Graphite, wt.%	Temperature range (°C)					% of char at 700 °C	LOI = 17.5 + 0.4(CY)	
		T_{initial}	Mass loss (%)	T_{max}	Mass loss (%)	T_{final}			
C-1	0	309	13.8	382	65.6	456	91.3	6.70	20.18
C-2	1	280	15.4	384	73.3	458	95.9	1.42	18.06
C-3	3	281	14.0	376	63.3	456	85.8	12.22	22.38
C-4	5	267	10.5	375	61.2	452	82.6	15.74	23.80

LOI indicates the slightest percentage volume of oxygen essential for the downward burning of a vertically mounted test sample. It is assessed in a nitrogen-oxygen mixture. This arithmetic index is widely represented as LOI [51]. For pure rooflite resin designated as C-1, the LOI value assessed is 20.18%, which is less than 21%. For the composite designated as C-2 containing 1% graphite the assessed LOI value is 18.06%, which is lower. The lower the LOI values expressed, the higher the inflammability capacity of the materials subjected. Both pure rooflite resin and its graphite composite designated as C-1 which contains 1% graphite are considered to be inflammable. Similarly, the LOI values for the composites named C-3 and C-4 are 22.38% and 23.80%, respectively. These composites are considered self-extinguishable materials.

The fact that both pure resin and its composites express LOI values that are less than 21% and are considered inflammable is a major demerit [52]. For bipolar plates, 120 °C is considered to be the maximum operating temperature for ideal graphite composites, according to Department of Energy (DOE) of the United States of America 267 °C is the lowest temperature required for the decomposition of rooflite resin composite. In turn, because the rooflite resin graphite composites designated as C-3 and C-4 have LOI values above 21%, these materials can be regarded as self-extinguishable. Bipolar plates, which are an essential component of fuel cells, can be made from such fire-self-extinguishable materials.

3.6. Chemical resistance study

A study was conducted to evaluate the chemical resistance of composites against different solvents/solutions such as water, NaCl, NaOH, acetic acid, and toluene. The results are shown in Table 4. It is evident that practically all of the chemical reagents utilized in this investigation cause weight gain [53, 54]. According to the experimental findings, these hybrid composites might be employed to create chemical and water storage tanks [55]. Figure 10 showed a comparison of the weight changes of the graphite composites and pure rooflite resin. Graphite-reinforced rooflite resin composites showed different chemical resistance behavior in different chemical environments. In the case of acetic acid, pure rooflite resin showed a negligible increase in weight [56, 57]. However, for composites, it was observed that increasing weight with the increased graphite filler concentration reached the maximum for C-4. A similar trend is also witnessed for water. Filler graphite is hydrophilic, and hence the weight increases. When compared with water, acetic acid environment impacts the samples' weight to a lesser degree. The increasing weight of the specimen is directly proportional to the filler content in the composite which is vulnerable to the chemical attack resulting in decreased resistance towards water [58]. The best chemical resistance was observed towards the NaCl solution environment. Nevertheless, the absorption mass dependence for the NaCl solution behaved erratically, rising

and falling for the different filler percentages. The increasing absorption mass percentage is visualized for toluene. According to the chemical resistance investigation, graphite-reinforced composites were more resistant to acid than alkali solutions. The increased interaction between sodium hydroxide and graphite filler results in the decreased resistance observed here [58, 59]. This weight shift suggests that the chemical reagents are causing the rooflite composites to swell instead of dissolving [60]. When different solvent and solutions are employed as a corrosive environment, an increase in the weight of the rooflite resin and its graphite composites is seen. Water being a small molecule may fill the spaces in the polymer matrix due to the formation of the hydrogen bonding with the carbonyl groups found in the lattice of polymers, which is the cause of the weight gain. Likewise, acetic acid also forms hydrogen bonds with carbonyl groups, which causes the weight to rise. The amount of the weight gain is slightly less than that of water, albeit there may be a steric impediment due to bigger size. When considering sodium hydroxide, alkaline sodium replaces some of the acidic hydrogen's in the polymer matrix. As a result, a gain in weight was noticed. The same replacement is expected in case of NaCl, but since it is a neutral solution the magnitude is less when compared to sodium hydroxide. In case of toluene, due to π - π stacking interactions, the solvent molecules have an affinity towards the polymer matrix, and the weight increases.

Due to the introduction of graphite into the polymer matrix in lower concentrations, some interstices may be left empty within the polymer matrix, allowing the solvent molecules to penetrate into the polymer matrix. As a result, the weight gain is appreciable when graphite is introduced into the polymer matrix. However, when the graphite concentration increases it may occupy some of the interstices and prevents the entry of the solvent molecule, which is the reason for reduction in weight gain. This study on chemical resistance behavior made it clear that rooflite-graphite composites can be utilized in a variety of engineering sectors, including fuel cells.

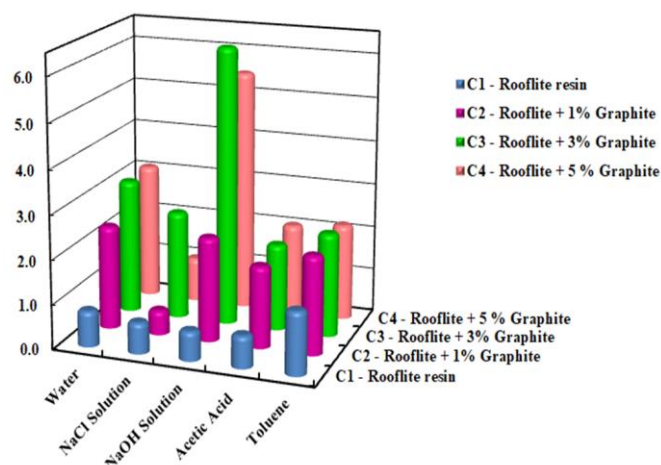


Figure 10 Change of weight percentage (%) in pure rooflite resin and its graphite composites due to various solvents.

Table 4 The change in mass percentage (%) by chemical environment.

Sample code	Water	NaCl solution	NaOH solution	Acetic acid	Toluene
C-1	0.8137%	0.7031%	0.6696%	0.7314%	1.4227%
C-2	2.3505%	0.5561%	2.3590%	1.8558%	2.2249%
C-3	3.0595%	2.4462%	6.3011%	1.9642%	2.3478%
C-4	3.0908%	1.0036%	5.4894%	2.0537%	2.1877%

4. Limitations

The research was undertaken to modify UPR to improve its mechanical, thermal, and chemical properties. However, incorporating fibers into the UPR matrix significantly improves the overall mechanical strength of the composites as compared to the pure polymer, which is yet to be studied.

5. Conclusions

In the present work the synthesis of rooflite unsaturated polyester resin and three of its composites with graphite containing 1%, 3% and 5% by weight (C-2, C-3 and C-4, respectively) were synthesised and characterised by FTIR, XRD studies, crystallinity, SEM, DSC, and thermogravimetric analysis. Chemical resistance investigation against water, NaCl, NaOH, acetic acid, and toluene was also carried out.

The crystallinity index of these composite materials increased due to the enhanced interaction between the resin matrix and filler graphite. Agglomeration takes place due to higher concentration of graphite filler which lowers the interfacial contact and affects the mechanical characteristics of the composites. The glass transition temperature increased with the addition of graphite. The synthetic composites exhibit a consistent swelling behavior in response to different chemical environments. The limiting oxygen index study revealed that the composites become self-extinguishing when the percentage of graphite is raised, suggesting that they could serve as fire self-extinguishable materials and could be further explored for making bipolar plates in fuel cells. Further graphite addition can enhance the thermal conductivity and widen the application of rooflite unsaturated polyester resin composites.

• Supplementary materials

No supplementary materials are available.

• Funding

This research had no external funding.

• Acknowledgments

The authors would like to thank the Principal, and Head of the department of Chemistry, Government Arts college, Udumalpet 642 126, for allowing us to conduct the experiments. We extend our thanks to Dr. R. Venckatesh, Department of Chemistry, Government Arts college, Udumalpet

642 126 for helping us in the IR spectral studies of the samples. The Authors wish to thank DST FIST DST-FIST-2018 (SR/FST/COLLEGE-417/2018) (TPN-2011) laboratory of the department for providing assistance to this research.

• Author contributions

Conceptualization: R.S., C.T.V.

Formal Analysis: M.K.

Supervision: R.S., C.T.V.

Writing – original draft: M.K.

Writing – review & editing: R.S., A.T., C.T.V.

• Conflict of interest

The authors declare no conflict of interest.

• Additional information

Author IDs:

M. Karunakaran, Scopus ID [36184086200](#);

Ravi Subban, Scopus ID [57062419500](#);

A. Thangamani, Scopus ID [22235774600](#);

Chinnaswamy Thangavel Vijayakumar, Scopus ID [7003381516](#).

Websites:

Department of Chemistry, Government Arts College, <https://www.gacudpt.in/index.php>;

Karpagam Academy of Higher Education, <https://kashedu.edu.in/>;

Kamaraj College of Engineering and Technology (Autonomous), <https://kamarajengg.irins.org/>.

References

- Mutar MA, Safi Khliwi F, Jameel Kamel R. Mechanical properties of new composite unsaturated polyesters based on nano fillers for marine application. *J Phys Conf Ser.* 2019;1294(5):052075. doi:[10.1088/1742-6596/1294/5/052075](#)
- Mohammed AJ, Razza HA. Study the effect of the adding the copper powder on the mechanical properties for unsaturated polyester. *J Sci Eng Res.* 2017;4(8):151.
- Gañán P, Barajas J, Zuluaga R, Castro C, Marín D, Tercjak A, Builes DH. The evolution and future trends of unsaturated polyester biocomposites: a bibliometric analysis. *Polymers (Basel).* 2023;15(13):2970. doi:[10.3390/polym15132970](#)
- Obayi CS, Odukwé AO, Obikwelu DON. Some tensile properties of unsaturated polyester resin reinforced with varying volume fractions of carbon black nanoparticles. *Niger J Technol.* 2008;27(1):20.
- Goudarzi R, Motlagh GH. An Insight into the diffusion of unsaturated polyester (UP) resin into Expanded Graphite (EG)

- to improve the mechanical properties of the UP/EG composites. *J Macromol Sci Part B*. 2020;59(8):502. doi:[10.1080/00222348.2020.1747231](https://doi.org/10.1080/00222348.2020.1747231)
6. Yavari N, Poorabdollah M, Rajabi L. Modified and unmodified Graphite/unsaturated polyester resin composites: thermal and mechanical behavior. *Iran J Chem Eng*. 2020;17(2):14. doi:[10.22034/ijche.2020.232609.1334](https://doi.org/10.22034/ijche.2020.232609.1334)
7. Swain S. Synthesis and characterization of graphene based unsaturated polyester resin composites. *Trans Electr Electron Mater*. 2013;14(2):53. doi:[10.4313/TEEM.2013.14.2.53](https://doi.org/10.4313/TEEM.2013.14.2.53)
8. Goudarzi R, Motlagh GH, Elhamnia M, Motahari S, Graphite nanosheet as low shrinkage additive, curing accelerator, and conducting filler for unsaturated polyester resin. *Polym Plast Technol Eng*. 2016;55(12):1231. doi:[10.1080/03602559.2015.1132468](https://doi.org/10.1080/03602559.2015.1132468)
9. Bastiurea M, Rodeanu Bastiurea MS, Andrei G, Dima D, Murarescu M, Ripa M, Circiumaru A. Determination of specific heat of polyester composite with graphene and graphite by differential scanning calorimetry. *Tribol Ind*. 2014;36(4):419. doi:[10.1016/j.biortech.2015.09.096](https://doi.org/10.1016/j.biortech.2015.09.096)
10. Segal L, Creely JJ, Martin AE, Conrad CM. An empirical method for estimating the degree of crystallinity of native cellulose using the X-Ray diffractometer. *Text Res J*. 1959;29(10):786.
11. Jiang L, Zheng A, Zhao Z, He F, Li H, Wu N. The comparison of obtaining fermentable sugars from cellulose by enzymatic hydrolysis and fast pyrolysis. *Bioresour Technol*. 2016;200:8. doi:[10.1016/j.biortech.2015.09.096](https://doi.org/10.1016/j.biortech.2015.09.096)
12. Dwyer JL, Zhou M, Polymer characterization by combined chromatography-infrared spectroscopy. *Int J Spectrosc*. 2011;1. doi:[10.1155/2011/694645](https://doi.org/10.1155/2011/694645)
13. Galpaya D, Wang M, George G, Motta N, Waclawik E, Yan C. Preparation of graphene oxide/epoxy nanocomposites with significantly improved mechanical properties. *J Appl Phys*. 2014;116(5):053518-1. doi:[10.1063/1.4892089](https://doi.org/10.1063/1.4892089)
14. Koto N, Soegijono B. Effect of rice husk ash filler of resistance against of high-speed projectile impact on polyester-fiberglass double panel composites. *J Phys Conf Ser*. 2019;1191:012058. doi:[10.1088/1742-6596/1191/1/012058](https://doi.org/10.1088/1742-6596/1191/1/012058)
15. Knežević N, Jovanović A, Bošnjaković J, Milošević M, Rančić M, Marinković A, J. Gržetić, H. Gamoudi, Fire-resistant composites based on acrylic-functionalized lignin and polyester resin obtained from waste poly(ethylene terephthalate). *Sci Tech Rev*. 2022;72(2):32. doi:[10.5937/str2202032K](https://doi.org/10.5937/str2202032K)
16. Lee UJ, Shin SR, Noh H, Song HB, Kim J, Lee DS, Kim BG. Rationally designed eugenol-based chain extender for self-healing polyurethane elastomers. *ACS Omega*. 2021;6(43):28848. doi:[10.1021/acsomega.1c03802](https://doi.org/10.1021/acsomega.1c03802)
17. Zięba-Palus J, The usefulness of infrared spectroscopy in examinations of adhesive tapes for forensic purposes. *Forensic Sci Criminol*. 2017;2(2):1. doi:[10.15761/FSC.1000112](https://doi.org/10.15761/FSC.1000112)
18. Reddy KO, Shukla M, Maheswari CU, Rajulu AV. Evaluation of mechanical behavior of chemically modified Borassus fruit short fiber/unsaturated polyester composites. *J Compos Mater*. 2012;46(23):2987. doi:[10.1177/0021998312454032](https://doi.org/10.1177/0021998312454032)
19. Bera M, Chandravati, Gupta P, Maji PK, Facile One-Pot Synthesis of graphene oxide by sonication assisted mechanochemical approach and its surface chemistry. *J Nanosci Nanotechnol*. 2018;18(2):902. doi:[10.1166/jnn.2018.14306](https://doi.org/10.1166/jnn.2018.14306)
20. Ruiz S, Tamayo JA, Ospina JD, Navia Porras DP, Valencia Zapata ME, Hernandez JHM, Valencia CH, Zuluaga F, Grande Tovar CD. Antimicrobial films based on nanocomposites of chitosan/poly(vinyl alcohol)/graphene oxide for biomedical applications. *Biomolecules*. 2019;9(3):109. doi:[10.3390/biom9030109](https://doi.org/10.3390/biom9030109)
21. Ban FY, Majid SR, Huang NM, Lim HN. Graphene oxide and its electrochemical performance. *Int J Electrochem Sci*. 2012;7:4345.
22. Isa MT, Ahmed AS, Aderemi O, Taib M, Mohammed-Dabo IA. Effect of dioctyl phthalate on the properties of unsaturated polyester resin. *Int J Mater Sci*. 2012;7(1):9.
23. Ambika MR, Nagaiah N, Harish V, Lokanath NK, Sridhar MA, Renukappa NM, Suman SK. Preparation and characterisation of Isophthalic-Bi₂O₃ polymer composite gamma radiation shields. *Radiat Phys Chem*. 2017;130:351. doi:[10.1016/j.radphyschem.2016.09.022](https://doi.org/10.1016/j.radphyschem.2016.09.022)
24. Pichaimani P, Arumugam H, Gopalakrishnan D, Krishnasam B, Muthukaruppan A. Partially exfoliated α -ZrP reinforced unsaturated polyester nanocomposites by simultaneous copolymerization and brønsted acid-base strategy. *J Inorg Organomet Polym Mater*. 2020;30(10):4095. doi:[10.1007/s10904-020-01558-x](https://doi.org/10.1007/s10904-020-01558-x)
25. Stanev V, Vesselinov V.V, Kusne AG, Antoszewski G, Takeuchi I, Alexandrov BS. Unsupervised phase mapping of X-ray diffraction data by nonnegative matrix factorization integrated with custom clustering. *Npj Comput Mater*. 2018;4(1):43. doi:[10.1038/s41524-018-0099-2](https://doi.org/10.1038/s41524-018-0099-2)
26. Maradini G, Oliveira M, Guanaes G, Passamani GZ, Carreira LG, Boschetti WTN, Monteiro SN, Pereira AC, de Oliveira BF. Characterization of polyester nanocomposites reinforced with conifer fiber cellulose nanocrystals polymers (Basel). 2020;12(12):2838. doi:[10.3390/polym12122838](https://doi.org/10.3390/polym12122838)
27. Wangn Y, Zhang M, Chang S, Li S, Huang X. Laser-induced ignition and combustion behavior of individual graphite micro-particles in a micro-combustor processes. 2020;8(11):1493. doi:[10.3390/pr8111493](https://doi.org/10.3390/pr8111493)
28. Gan L, Guo H, Wang Z, Li X, Peng W, Wang J, Huang S, Su M. A facile synthesis of graphite/silicon/graphene spherical composite anode for lithium-ion batteries. *Electrochim Acta*. 2013;104:117. doi:[10.1016/j.electacta.2013.04.083](https://doi.org/10.1016/j.electacta.2013.04.083)
29. Braga NF, Passador FR, Saito E, Cristovan FH. Effect of graphite content on the mechanical properties of Acrylonitrile-Butadiene-Styrene (ABS). *Macromol Symp*. 2019;383(1):1800018. doi:[10.1002/masy.201800018](https://doi.org/10.1002/masy.201800018)
30. Zhou L, Zhou R, Zuo J, Tu S, Yin Y, Ye L. Unsaturated polyester resins with low- viscosity: preparation and mechanical properties enhancement by isophorone diisocyanate (IPDI) modification. *Mater Res Express*. 2019;6(11):115305. doi:[10.1088/2053-1591/ab4380](https://doi.org/10.1088/2053-1591/ab4380)
31. Feng L, Li R, Yang H, Chen S, Yang W. The hyperbranched polyester reinforced unsaturated polyester resin. *Polymers (Basel)*. 2022;14(6):1127. doi:[10.3390/polym14061127](https://doi.org/10.3390/polym14061127)
32. Heo SI, Yun JC, Oh KS, Han KS. Influence of particle size and shape on electrical and mechanical properties of graphite reinforced conductive polymer composites for the bipolar plate of PEM fuel cells. *Adv Compos Mater*. 2006;15(1):115. doi:[10.1163/156855106776829356](https://doi.org/10.1163/156855106776829356)
33. Alghamdi AS, Ashcroft IA, Song M. Creep resistance of novel Polyethylene/Carbon Black nanocomposites. *Int J Mater Sci Eng*. 2014;15:16. doi:[10.12720/ijmse.2.1.1-5](https://doi.org/10.12720/ijmse.2.1.1-5)
34. Ukoba KO, Inambao FL, Eloka-Eboka AC. Fabrication of Affordable and sustainable solar cells using NiO/TiO₂ P - N Heterojunction. *Int J Photoenergy*. 2018;2018:1. doi:[10.1155/2018/6062390](https://doi.org/10.1155/2018/6062390)
35. Dusevich VM, Purk JH, Eick JD, Choosing the Right Accelerating Voltage for SEM (An Introduction for Beginners). *Microsc Today*. 2010;18(1):48. doi:[10.1017/S1551929510991190](https://doi.org/10.1017/S1551929510991190)
36. Hapke J, Gehrig F, Huber N, Schulte K, Lilleodden ET. Compressive failure of UD-CFRP containing void defects: In situ SEM microanalysis *Compos Sci Technol*. 2017;71(1):1242. doi:[10.1016/j.compscitech.2011.04.009](https://doi.org/10.1016/j.compscitech.2011.04.009)
37. Abdul Khalil HPS, Tye YY, Ismail Z, Leong JY, Saurabh CK, Lai TK, Chong EWN, Aditiawati P, Tahir PM, Dungani R. Oil palm shell nanofiller in seaweed-based composite film: Mechanical, Physical, and Morphological Properties. *BioResources*. 2017;12(3):5996. doi:[10.15376/biores.12.3.5996-6010](https://doi.org/10.15376/biores.12.3.5996-6010)
38. Bing N, Yang J, Gao H, Xie H, Yu W. Unsaturated polyester resin supported form-stable phase change materials with enhanced thermal conductivity for solar energy storage and conversion. *Renew Energy*. 2021;173:926. doi:[10.1016/j.renene.2021.04.033](https://doi.org/10.1016/j.renene.2021.04.033)
39. Bastiurea M, Bastiurea MS, Andrei G, Murarescu M, Dumitru D. Determination of Glass Transition Temperature for Polyester / Graphene Oxide and Polyester / Graphite Composite by TMA and DSC. *Metall Mater Sci*. 2015;38(2):32.

40. Jaya Vinse Ruban Y, Ginil Mon S, Vetha Roy D. Chemical resistance/thermal and mechanical properties of unsaturated polyester-based nanocomposites. *Appl Nanosci*. 2014;4(2):233. doi:[10.1007/s13204-013-0193-1](https://doi.org/10.1007/s13204-013-0193-1)
41. Jia W, Tchoudakov R, Narkis M, Siegmann A, Performance of expanded graphite and expanded milled-graphite fillers in thermosetting resins. *Polym Compos*. 2005;26(4):526. doi:[10.1002/pc.20123](https://doi.org/10.1002/pc.20123)
42. Bastiurea M, Rodeanu MS, Andrei G, Dima D, Cantaragiu A. Correlation between graphene oxide / graphite content and thermal properties of polyester composites. *Dig J Nanomater Biostructures*. 2015;10(4):1109.
43. Cherian AB, Varghese LA, Thachil ET, Epoxy-modified, unsaturated polyester hybrid networks. *Eur Polym J*. 2007;43(4):1460. doi:[10.1016/j.eurpolymj.2006.12.041](https://doi.org/10.1016/j.eurpolymj.2006.12.041)
44. Magampa PP, Manyala N, Focke WW. Properties of graphite composites based on natural and synthetic graphite powders and a phenolic novolac binder. *J Nucl Mater*. 2013;436(1-3):76. doi:[10.1016/j.jnucmat.2013.01.315](https://doi.org/10.1016/j.jnucmat.2013.01.315)
45. Bastiurea M, Rodeanu MS, Dima D, Murarescu M, Andrei G. Thermal and mechanical properties of polyester composites with graphene oxide and graphite. *Dig J Nanomater Biostructures*. 2015;10(2):521.
46. Kandare E, Kandola BK, Price D, Nazaré S, Horrocks RA. Study of the thermal decomposition of flame-retarded unsaturated polyester resins by thermogravimetric analysis and Py-GC/MS. *Polym Degrad Stab*. 2008;93(11):1996. doi:[10.1016/j.polymdegradstab.2008.03.032](https://doi.org/10.1016/j.polymdegradstab.2008.03.032)
47. Tibiletti L, Longuet C, Ferry L, Coutelen P, Mas A, Robin JJ, Lopez-Cuesta JM. Thermal degradation and fire behaviour of unsaturated polyesters filled with metallic oxides. *Polym Degrad Stab*. 2011;96(1):67. doi:[10.1016/j.polymdegradstab.2010.10.015](https://doi.org/10.1016/j.polymdegradstab.2010.10.015)
48. Dai K, Song L, Hu Y. Study of the flame retardancy and thermal properties of unsaturated polyester resin via incorporation of a reactive cyclic phosphorus-containing monomer. *High Perform Polym*. 2013;25(8):938. doi:[10.1177/0954008313490767](https://doi.org/10.1177/0954008313490767)
49. Ramadan N, Taha M, La Rosa AD, Elsabbagh A. Towards selection charts for epoxy resin, unsaturated polyester resin and their fibre-fabric composites with flame retardants. *Mater*. 2021;14(5):1181. doi:[10.3390/ma14051181](https://doi.org/10.3390/ma14051181)
50. Laoutid F, Bonnaud L, Alexandre M, Lopez-Cuesta JM, Dubois P. New prospects in flame retardant polymer materials: From fundamentals to nanocomposites *Mater Sci Eng R Reports*. 2009;63(3):100. doi:[10.1016/j.mser.2008.09.002](https://doi.org/10.1016/j.mser.2008.09.002)
51. Ranganathan T, Beaulieu M, Zilberman J, Smith KD, Westmoreland PR, Farris RJ, Coughlin EB, Emrick T. Thermal degradation of deoxybenzoin polymers studied by pyrolysis-gas chromatography/mass spectrometry. *Polym Degrad Stab*. 2008;93(6):1059. doi:[10.1016/j.polymdegradstab.2008.03.021](https://doi.org/10.1016/j.polymdegradstab.2008.03.021)
52. Dai K, Song L, Jiang S, Yu B, Yang W, Yuen RKK, Hu Y. Unsaturated polyester resins modified with phosphorus-containing groups: Effects on thermal properties and flammability *Polym Degrad Stab*. 2013;98(10):2033. doi:[10.1016/j.polymdegradstab.2013.07.008](https://doi.org/10.1016/j.polymdegradstab.2013.07.008)
53. Noorunnisa Khanam P, Abdul Khalil HPS, Jawaaid M, Ramachandra Reddy G, Surya Narayana C, Venkata Naidu S. Sisal/Carbon fibre reinforced hybrid composites: tensile, flexural and chemical resistance properties. *J Polym Environ*. 2010;18(4):727. doi:[10.1007/s10924-010-0210-3](https://doi.org/10.1007/s10924-010-0210-3)
54. Ramamoorthi R, Sampath PS. Experimental investigation of influence of Halloys nanotubes on mechanical and chemical resistance properties of glass fiber reinforced epoxy non composites. *J Sci Ind Res*. 2015;74:685.
55. Ashok Kumar M, Hemachandra Reddy K, Ramachandra Reddy G, Venkata Mohana Reddy Y, Subbarami Reddy, Tensile, thermal properties & chemical resistance of epoxy/hybrid fibre composites (Glass/Jute) filled with silica powder. *Macromol Indian J*. 2010;6(2):133.
56. Tasnim S, Uddin Ahmed Shaikh F. Effect of chemical exposure on mechanical properties and microstructure of lightweight polymer composites containing solid waste fillers. *Constr Build Mater*. 2021;309:125192. doi:[10.1016/j.conbuildmat.2021.125192](https://doi.org/10.1016/j.conbuildmat.2021.125192)
57. Singha AS, Thakur VK. Chemical resistance, mechanical and physical properties of biofibers -based polymer composites. *Polym Plast Technol Eng*. 2009;48(7):736. doi:[10.1080/03602550902824622](https://doi.org/10.1080/03602550902824622)
58. Hazarika A, Maji TK. Study on the properties of wood polymer nanocomposites based on melamine formaldehyde-furfuryl alcohol copolymer and modified clay. *J Wood Chem Technol*. 2013;33(2):103. doi:[10.1080/02773813.2012.751428](https://doi.org/10.1080/02773813.2012.751428)
59. Mandal M, Halim Z, Maji TK. Mechanical, moisture absorption, biodegradation and physical properties of nanoclay-reinforced wood/plant oil composites *SN Appl Sci*. 2020;2(2):250. doi:[10.1007/s42452-020-1984-0](https://doi.org/10.1007/s42452-020-1984-0)
60. Karthikeyan SKS, Sujatha MSM, Hemalatha NHN. Synthesis and characterization of multi-walled carbon nanotube from pine oil and their impact on carbon fibre reinforced epoxy hybrid nanocomposite. *J Environ Nanotechnol*. 2021;10(2):10. doi:[10.13074/jent.2021.06.212437](https://doi.org/10.13074/jent.2021.06.212437)